# Identification of a Nonlinear Aeroelastic Aircraft Wing Model

Christopher M. Richards*
*University of Louisville, Louisville, Kentucky 40292*
Martin J. Brenner†
*NASA Dryden Flight Research Center, Edwards, California 93523*
and
Rajendra Singh‡
*The Ohio State University, Columbus, Ohio 43210*

**The "reverse path" spectral method, a frequency domain based nonlinear system identification technique, is considered for identifying nonlinear aeroelastic models. The method is based upon a multi-input/multi-output spectral conditioning process that mutually uncorrelates the linear and nonlinear components of the system response. Conditioned frequency response estimates derived from this process enable estimation of the system's underlying linear frequency response matrix without contaminating effects from the nonlinearities. Analytic functions for describing the system's nonlinearities are also identified once the linear frequency response matrix has been estimated. Since these analytic functions must be chosen prior to the identification, conditioned coherence functions, also derived from the spectral conditioning process, are used to indicate the presence (or absence) of select nonlinear components in the response data, hence overcoming the *a priori* assumption of this and many other parametric-based nonlinear system identification techniques. To illustrate the performance of the identification method, numerical data is first simulated from a nonlinear analytical aeroelastic system. Results show that the method is capable of identifying an accurate nonlinear aeroelastic model even when the underlying nonlinearities are unknown. The usefulness of the conditioned coherence functions for selecting analytic functions for describing the nonlinearities is also illustrated. The method is then applied to test data collected from the Active Aeroelastic Wing (AAW) aircraft, an experimental vehicle used to investigate active flexibility control of aircraft wings for improved maneuverability, weight reduction and extended range.**

## I. Introduction

Accuracy of analytical/experimental hybrid based flutter prediction tools depends on the underlying aeroelastic models that are identified from experimental flight data[1]. Developing an accurate aeroelastic model is often complicated by nonlinear dynamic behavior observed from the experimental data[2,3]. This behavior can be the result of various structural and flow sources, including piecewise linear stiffness resulting from structural discontinuities, nonlinear stiffness arising from large wing displacements and aerodynamic flows with large shock motions and flow separation[4,5]. Therefore, nonlinear system identification techniques are necessary in order to take into account the presence of these types of nonlinearities and others[6].

There have been a number of approaches used for identifying nonlinear systems in the recent years[2,3,7,8]. For instance, wavelets have shown to be successful for describing polynomial type nonlinearities of an aeroelastic model

* Assistant Professor, Department of Mechanical Engineering. Member AIAA.

† Aerospace Engineer, Aerostructures Branch, MS 4840D/RS. Member AIAA.

‡ Donald D. Glower Chair. Department of Mechanical Engineering.

as well as predict the limit-cycle oscillation of the same system using time-frequency maps generated from the wavelet analysis[7]. Wavelets have also been used in conjunction with singular-value decomposition, transformed-singular-value decomposition and wavelet based modal parameter estimation for extracting modal parameters from non-stationary data[8]. Data considered were simulated sinusoidal signals, data from a test-bed nonlinear aeroelastic system, aeroelastic flight data from a drone flutter experiment and data from an F18 flight test. The methods, one using the singular-value decomposition and the other using transformed-singular-value decomposition, provided promising results for all for data cases considered. In addition, the Volterra series has been employed to identify nonlinear aeroelastic systems where the first order Volterra kernel, which is the linear component of the system response, is used to improve flutter prediction accuracy by uncertainty estimation[2].

In this study, the "Reverse Path" Spectral Method (RPSM), a frequency domain based nonlinear system identification technique, is considered[9,10]. The RPSM utilizes conditioned coherence functions to indicate the presence of selected nonlinear components in the response data and to indicate the overall accuracy of the identification model. The method is first evaluated using numerically simulated data from an analytical aeroelastic model and is then applied to test data collected from the Active Aeroelastic Wing (AAW) aircraft[11].

## II. Background

Conventional frequency response estimation methods such as the "$H_1$" and "$H_2$" methods[12] often yield frequency response functions that are contaminated by the presence of nonlinearities and hence make it difficult or impossible to extract underlying linear system properties from measured multi-input/multi-output (MIMO) experimental data[13]. To overcome this difficulty, a spectral approach for identifying multi-degree-of-freedom nonlinear systems, known as the "Reverse Path" Spectral Method (RPSM), has been developed[9]. The method calculates a conditioned frequency response matrix $\mathbf{H}(\omega)$ without contaminating effects from the nonlinearities. In addition, functions for describing the system's nonlinearities are also identified. Derivation of the method begins with the set of coupled frequency domain nonlinear equations of motion for describing an $N$ input, $M$ output vibratory system with $n$ nonlinearities:

$$\mathbf{B}(\omega)\mathbf{X}(\omega) + \sum_{j=1}^{n} \mathbf{a}_j Y_j(\omega) = \mathbf{F}(\omega) \tag{1}$$

where $\omega$ is frequency, $\mathbf{F}(\omega)$ is a vector containing the spectra of the externally applied excitations, $\mathbf{X}(\omega)$ is a vector of the system response spectra and $\mathbf{B}(\omega)$ is the system's linear dynamic stiffness matrix. The spectra $Y_j(\omega)$ are Fourier transforms of nonlinear functions $y_j(\mathbf{x}(t))$ that are included to describe the nonlinearities and the vectors $\mathbf{a}_j$ contain coefficients of these terms. The goal of the RPSM is to identify the underlying linear frequency response matrix $\mathbf{H}(\omega)$ ($\mathbf{H}(\omega) = \mathbf{B}(\omega)^{-1}$) of the system without influences from the nonlinearities, and identify the coefficients of the nonlinear functions contained in the vectors $\mathbf{a}_j$. To achieve this goal, a "reverse path" spectral model as shown in Figure 1(a) is derived by re-arranging equation (1) with $\mathbf{F}(\omega)$ as the output and $\mathbf{X}(\omega)$ and $Y_j(\omega)$ as the inputs to the model. Using spectral conditioning techniques[14], an equivalent conditioned "reverse path" model is determined and the "reverse path" model of Figure 1(a) can be redrawn as a model with uncorrelated inputs as shown in Figure 1(b), where the inputs $Y_{j(-1:j-1)}$ and $\mathbf{X}_{(-1:n)}$ are mutually uncorrelated (note, the dependence on $\omega$ has been dropped for the sake of brevity). The subscript in parentheses $(-1:j-1)$ indicates that that spectrum is uncorrelated with spectra $Y_1$ through spectra $Y_{j-1}$. Notice that the path between $\mathbf{X}_{(-1:n)}$ and $\mathbf{F}_{(-1:n)}$ remains unaltered from the conditioning process. This path is the linear dynamic stiffness matrix $\mathbf{B}$ and its input and output vectors are uncorrelated with all of the spectra of the nonlinear functions (the subscript $(-1:n)$ indicates that the respective vector is uncorrelated with all of the nonlinearities $Y_1$ through $Y_n$). Therefore, the underlying linear system can be identified without corruption from the nonlinearities. Since $\mathbf{H}$ is desired for modal parameter estimation, the linear path is re-reversed as illustrated in Figure 1(c). Now, any of the conventional frequency response estimation methods can be modified to estimate $\mathbf{H}$. For instance, the conditioned "$H_{c2}$" estimate is:

$$\mathbf{H}^T = \mathbf{G}_{XF(-1:n)}^{-1} \mathbf{G}_{XX(-1:n)} \tag{2}$$

where calculations for the conditioned power-spectral density (PSD) matrices $\mathbf{G}_{XX(-1:n)}$ and $\mathbf{G}_{XF(-1:n)}$ are derived in Ref. 9. Once $\mathbf{H}$ has been estimated, the coefficient vectors $\mathbf{a}_j$ can also be estimated (see Ref. 9 for development and solution). In addition, coherence functions have been formulated for the conditioned model of Figure 1(b)[10]:

$$\gamma^2_{jF(-1:j-1)} = \frac{\left|G_{jF(-1:j-1)}\right|^2}{G_{jj(-1:j-1)}G_{FF}}, 1 \le j \le n;\ \gamma^2_{X_iF(-1:n)} = \frac{\left|G_{X_iF(-1:n)}\right|^2}{G_{X_iX_i(-1:n)}G_{FF}},\ i = 1, N \tag{3a,b}$$

Equation (3a) is the coherence function for each of the nonlinear paths of the uncorrelated input model (i.e., the coherence between the inputs $Y_{j(1:j-1)}$ and the output $F$ where $F$ is one of the externally applied excitations). Equation (3b) is the coherence function for each element of $\mathbf{X}_{(-1:n)}$ and $F$. These coherence functions yield values from zero to one indicating the correlation between each input and output of the conditioned model. From these coherence functions the overall accuracy of the model is assessed by calculating the cumulative coherence for the system:

$$\gamma^2_{Mi}(\omega) = \gamma^2_{X_iF_1(-1:n)}(\omega) + \gamma^2_{YF_1}(\omega),\ i = 1, N;\ \gamma^2_{YF_1}(\omega) = \sum_{j=1}^{n}\gamma^2_{jF_1(-1:j-1)}(\omega) \tag{4a,b}$$

Since all of the inputs of the conditioned model are uncorrelated, the cumulative coherence, which is the sum of all of the input/output coherences, also maintains values between zero and one with values close to unity at frequencies that the model is accurate and values close to zero at frequencies that the model is inaccurate.

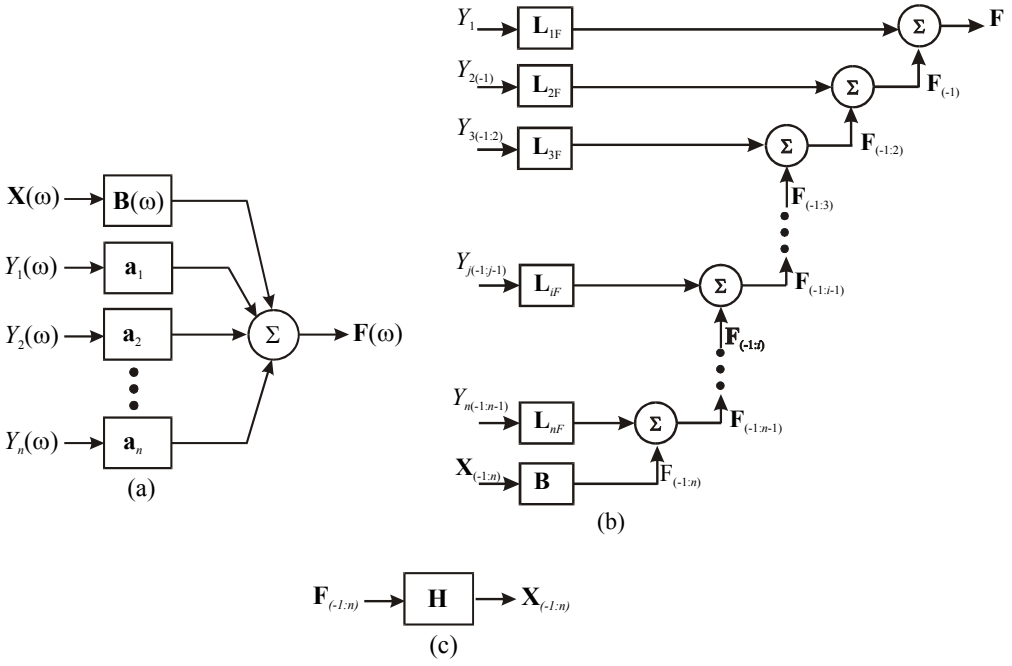


Figure 1. "Reverse path" system model. (a) correlated input form. (b) uncorrelated input form. (c) "forward path" of underlying linear system.

## III. Analytical Study

In this section an analytical aeroelastic model is developed to evaluate the performance of the RPSM. The model adopted for this evaluation is the two-degree-of-freedom pitch-plunge airfoil illustrated in Figure 2, where the translational and rotational structural stiffnesses of the wing are described by nonlinear functions $g(x)$ and $g_\alpha(x)$,

respectfully. For the coordinate system chosen (i.e., translational degree-of-freedom measured at the center-of-gravity), the elastically coupled, inertially uncoupled equations of motion are,

$$
\begin{aligned}
&\mathbf{M}\ddot{\mathbf{x}} + (\mathbf{C} + U\mathbf{L})\dot{\mathbf{x}} + (\mathbf{K} + U^2\mathbf{H})\mathbf{x} + \sum_{j=1}^{n} \mathbf{a}_j y_j(\mathbf{x}) = \mathbf{b} f_a; \\
&\mathbf{x} = \begin{bmatrix} w \\ \alpha \end{bmatrix}, \quad \mathbf{b} = \begin{bmatrix} 1 \\ -c_a \end{bmatrix}, \quad \mathbf{M} = \begin{bmatrix} m & 0 \\ 0 & I \end{bmatrix}, \quad \mathbf{C} = \beta\mathbf{K}, \\
&\mathbf{K} = \begin{bmatrix} k & -kc_e \\ -kc_e & k_\alpha + kc_e^2 \end{bmatrix}, \; \mathbf{H} = \frac{\rho c}{2}\frac{dC_L}{d\alpha}\begin{bmatrix} 0 & 1 \\ 0 & c(\frac{1}{4} - \frac{c_o}{c}) \end{bmatrix}, \\
&\mathbf{L} = \frac{\rho c}{2}\frac{dC_L}{d\alpha}\begin{bmatrix} 1 & c(\frac{3}{4} - \frac{c_o}{c}) \\ c(\frac{1}{4} - \frac{c_o}{c}) & c^2[(\frac{1}{4} - \frac{c_o}{c})(\frac{3}{4} - \frac{c_o}{c}) + \frac{\pi}{8}\Big/\frac{dC_L}{d\alpha}] \end{bmatrix}
\end{aligned}
\tag{5}
$$

where $m$ and $I$ are the mass and mass moment of inertia about the center of gravity of the wing, $\beta$ is the proportionality constant for this proportionally damped system, and $k$ and $k_\alpha$ are the coefficients of the linear terms of $g(w)$ and $g_\alpha(\alpha)$, respectfully. The derivative dCL/d$\alpha$ is assumed to be constant equal to $2\pi$, $U$ is the airspeed velocity and $\rho$ is the density of air. The external force $f_a$ is from aileron excitation as described later. The nonlinear functions $y_j(\mathbf{x})$ are made up of the nonlinear terms of $g(w)$ and $g_\alpha(\alpha)$. For a detailed description of how to develop these equations see Ref. 9. These physical parameters as well as the geometric parameters depicted in Figure 2 have been chosen to yield the "at rest" ($U = 0$) modal parameters listed in Table 1, where $f_r$ is the undamped natural frequency, $\zeta_r$ is the damping ratio and $\phi_r$ is the mode shape of the $r^{\text{th}}$ mode. For this evaluation study, $U$ was chosen to be $U_f/3$ where $U_f$ is the flutter speed.

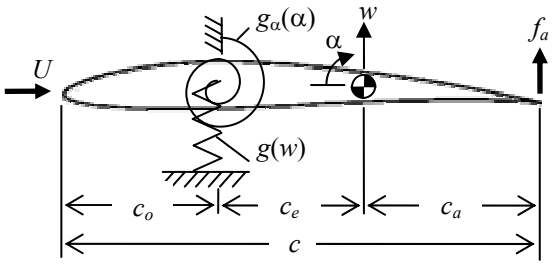

Figure 2. Analytical model.

| $r$ | $f_r$ (Hz) | $\zeta_r$ | $\phi_r$ |
|---|---|---|---|
| 1 | 14.20 | 0.02 | [ 1 0.05 ]$^T$ |
| 2 | 31.91 | 0.05 | [ -0.02 1 ]$^T$ |

Table 1. Modal parameters of the analytical aeroelastic model for $U = 0$.

The experimental component of the RPSM system identification process involves applying measurable external excitations, in this case the force $f_a$ generated by aileron excitation, and measuring the resulting system response, i.e., the translation $w$ and rotation $\alpha$ for this example. Since the purpose of this study is to evaluate the performance of the RPSM for use on experimental data collected on the AAW, the same type of excitation used during AAW experimental flights is used in this performance evaluation. The excitation applied to the AAW during flight consisted of Schroeder sweep[15,16] commands given to the ailerons while simultaneous measurements of aileron displacement and acceleration response of the aircraft wings were recorded (among many other measurements). To emulate a similar experiment for this analytical system, the AAW's right aileron displacement measurement multiplied by a gain is used here as the excitation $f_a$.

First consider an aircraft wing with linear structural torsional stiffness ($g_\alpha(\alpha) = k_\alpha\alpha$) and asymmetric hardening translational stiffness given by

$$g(w) = kw + a_1w^2 + a_2w^3 \tag{6}$$

where the coefficients of the nonlinear terms are $a_1$ = 1 MN/m$^2$ and $a_2$ = 100 MN/m$^3$. Also, initially assume that the types of the nonlinearities that make up the translational stiffness are known. Therefore, for equation (1) and the "reverse path" identification model depicted in Figure 1(a),

$$y_1(\mathbf{x}) = w^2, \quad y_2(\mathbf{x}) = w^3, \quad \mathbf{a}_1 = \begin{bmatrix}\hat{a}_1 & 0\end{bmatrix}^T, \quad \mathbf{a}_2 = \begin{bmatrix}\hat{a}_2 & 0\end{bmatrix}^T \tag{7a-d}$$

where $\hat{a}_1$ and $\hat{a}_2$ are estimates of $a_1$ and $a_2$, respectfully. The goal of the RPSM is to 1) estimate the linear frequency response functions (matrix **H**) of the wing so that the underlying modal parameters of the wing can be determined by modal parameter estimation techniques[17] and 2) yield accurate estimates $\hat{a}_1$ and $\hat{a}_1$ of the actual values for $a_1$ and $a_2$. After carrying out the necessary spectral conditioning, equation (2) determines the "$H_{c2}$" frequency response estimates. The estimates are shown in Figure 3 along with the actual underlying linear frequency response functions derived from equation (5) with $a_j = 0, j\in[1,n]$ as well as estimates by the conventional "$H_1$" frequency response estimation technique[12]. By comparing these results, it is apparent that modal parameter estimation would yield erroneous modal parameters from the conventional "$H_1$" estimated FRFs. However, since the "$H_{c2}$" estimate closely matches the actual underlying linear frequency response functions, accurate modal parameter estimation of the "$H_{c2}$" estimates would result.

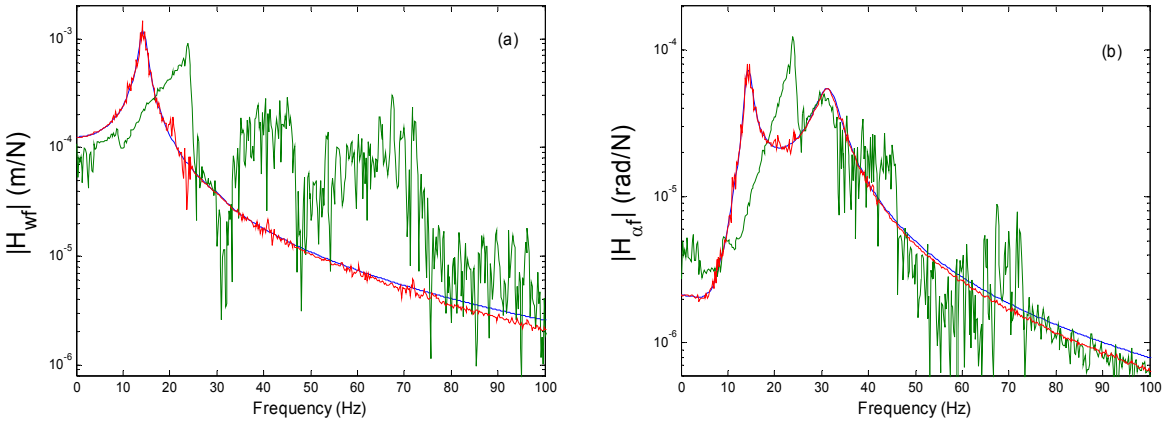


Figure 3. Magnitude of frequency response functions (FRFs). (a) FRF of wing translation to aileron excitation. (b) FRF of wing rotation to aileron excitation. —, actual FRF; —, conventional estimate; —, conditioned estimate.

Figure 4 is a graph of the conventional coherence function, which provides an indication of the accuracy of the "$H_1$" estimate, as well as the cumulative coherence function (equation (4a)), which indicates the accuracy the "$H_{c2}$" estimate. As illustrated, the cumulative coherence is much closer to unity than the conventional unconditioned coherence, indicating that the multi-input/output "reverse path" model with the proper nonlinear functions chosen as inputs is more accurate than a linear model whose inputs and outputs are the original unconditioned excitation and nonlinear response. Consequently, under "real-world" conditions in which the actual underlying frequency response functions are unknown, the cumulative coherence is a useful tool for evaluating the accuracy of the "reverse path" model.

Estimates $\hat{a}_1$ and $\hat{a}_2$ of the coefficients of the nonlinearities are plotted in Figure 5(a, b). Although the actual values $a_1$ and $a_2$ are constants and not a function of frequency, their estimates $\hat{a}_1$ and $\hat{a}_2$ are frequency dependent since all of the terms in the equation for determining these estimates are frequency dependent[9]. Therefore, accurate estimates of constant coefficients should not vary much with frequency, which is the case illustrated in the figures.

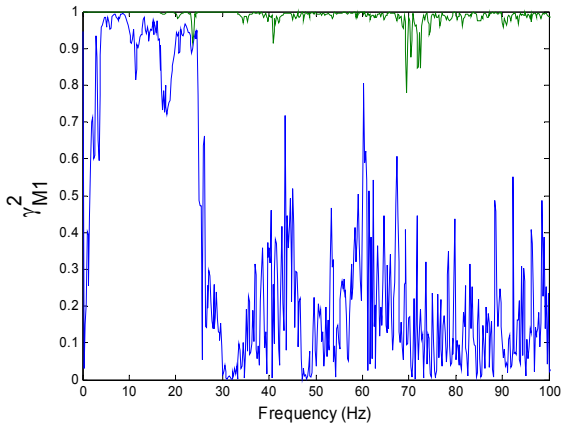


Figure 4. Coherence functions for estimates of $H_{wf}$. —, conventional coherence for "$H_1$" estimate; —, cumulative coherence for "$H_{c2}$" estimate.

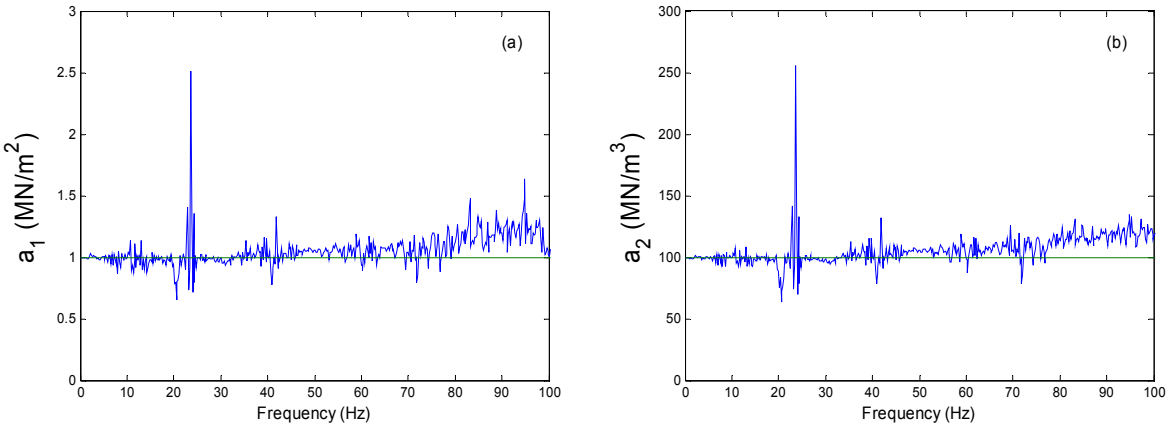


Figure 5. Coefficients of nonlinear stiffness terms. (a) quadratic term. (b) cubic term. —, estimate ; —, actual.

The assumption that the types of system nonlinearities that exist is known prior to the identification is unrealistic for most practical systems. Therefore, to extend this evaluation, consider now a nonlinear translational stiffness of the form,

$$g(w) = kw + a_1 \mathrm{sgn}(w) \cdot w^{\beta} \tag{8}$$

where β is an unknown non-integer power. For simulation of the system response, a value of β = 2.4 is chosen. However, from a system identification standpoint, it is unlikely for this type of nonlinearity to be chosen *a priori* for describing the wing's nonlinear translational stiffness. Instead, it is common practice to consider an approximation to the unknown nonlinearity such as an $m^{\text{th}}$ order truncated power series,

$$g(w) = kw + \sum_{j=1}^{m} a_j w^{j+1} \tag{9}$$

Using this equation to model the nonlinear translational stiffness, for equation (1) and the reverse path model depicted in Figure 1(a):

$$y_j(\mathbf{x}) = w^{j+1}, \quad \mathbf{a}_j = \begin{bmatrix} \hat{a}_j & 0 \end{bmatrix}^T \tag{10a-d}$$

Considering different values of $m$, spectral conditioning is carried out and equation (2) is employed to determine the "$H_{c2}$" frequency response estimates. Results are shown in Figure 6 along with the actual FRFs. To illustrate the strength of the nonlinearity and its detrimental effects on conventional frequency response estimation, an "$H_1$" estimate is shown in Figure 6(a).

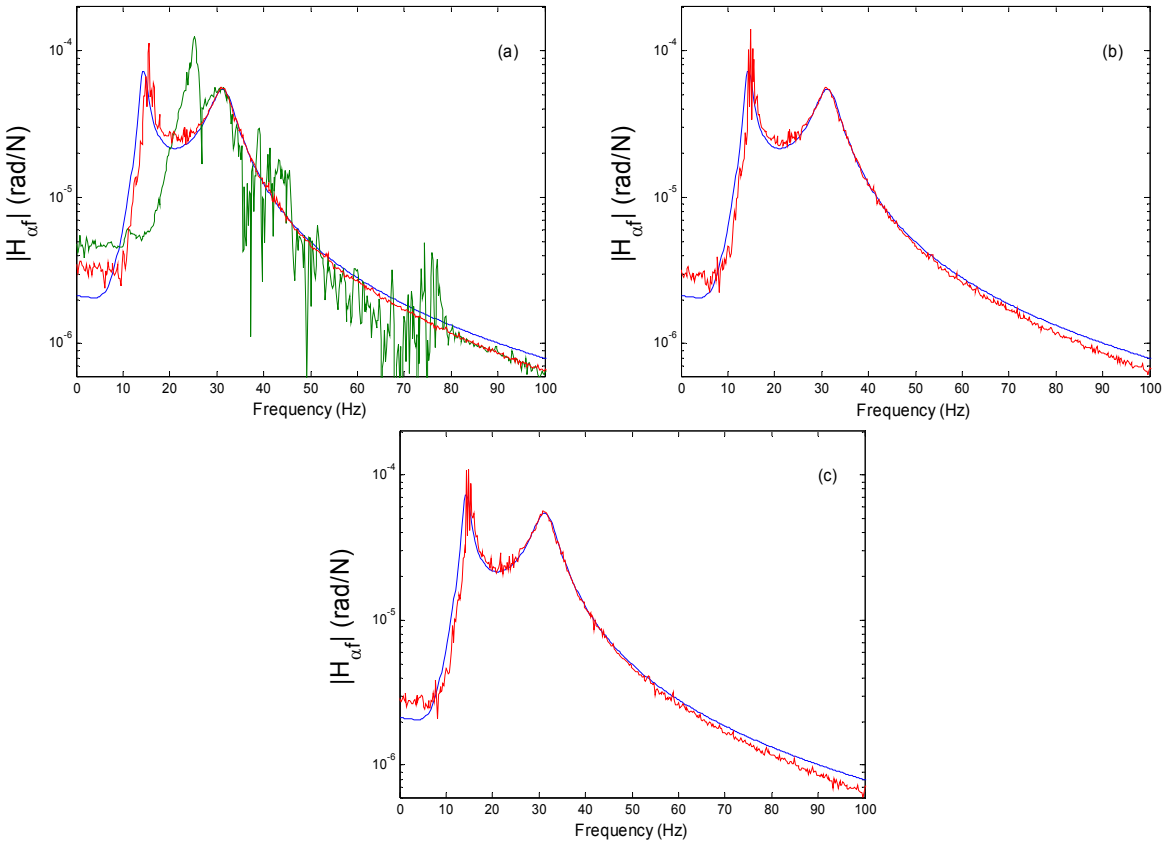


Figure 6. Magnitude of $H_{\alpha f}$ FRFs. (a) $m = 2$. (b) $m = 3$. (c) $m = 4$. —, actual FRF; —, conventional estimate; —, conditioned estimate.

For $m = 2$ a significant improvement of the frequency response estimation by the "$H_{c2}$" method over the conventional "$H_1$" method has been made. However, the first mode of the "$H_{c2}$" estimate is shifted slightly higher in frequency than the first mode of the actual underlying linear frequency response. This is likely due to the fact that the truncated series for $m = 2$ is an incomplete representation of the hardening stiffness nonlinearity given by equation (8) and therefore some remaining nonlinear effects are present in the estimation. Additional terms, $m = 3$ and $m = 4$, do however slightly improve the estimate.

Figure 7 are plots of the coefficients of the terms for $m = 2$. Notice from Figure 7(a) that the estimated coefficient for the quadratic term fluctuates about zero whereas the estimated coefficient for the cubic term fluctuates about 5 MN/m$^3$. Consequently, the quadratic term does not play a significant role in describing the nonlinearity. This is consistent with the fact that the actual nonlinearity is symmetric and therefore even order terms of the series add little to no value to the approximation.

As a further verification, consider the additional approximations, $m = 1$, and $m = 2, j \neq 1$. In other words, consider two additional models, one consisting only of a quadratic term and the other consisting only of a cubic term. Cumulative coherence functions for these two models and the $m = 2$ model are shown in Figure 8 (note, in

order to clearly illustrate the differences between the coherence functions, they are plotted on a scale from 0.8 to 1). As the figure illustrates, the coherence for the $m = 2$, $j \neq 1$ model is similar to the $m = 2$ model, indicating that the quadratic term in the $m = 2$ model adds little value to the estimation.

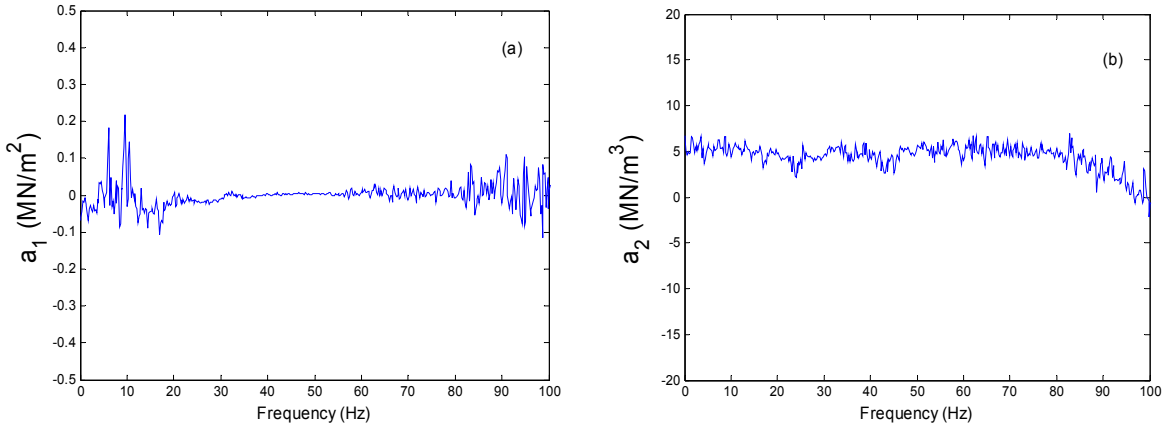


Figure 7. Coefficients of nonlinear stiffness terms. (a) quadratic term. (b) cubic term.

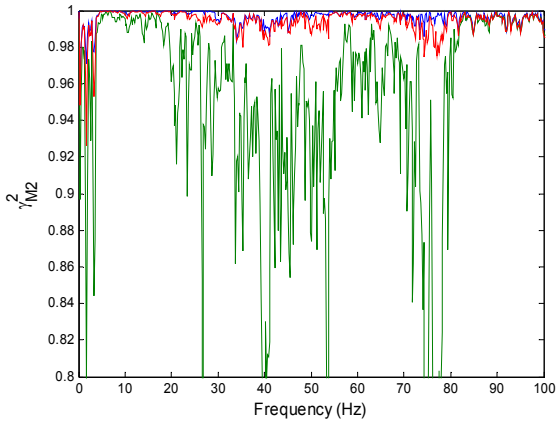


Figure 8. Cumulative coherence functions for "$H_{c2}$" estimates of $H_{\alpha f}$. —, $m = 2$ model; —, $m = 1$ model; —, $m = 2, j \neq 1$ model.

From this analysis, one might conclude that even ordered terms are unnecessary for the system identification. Therefore, consider now the odd-order-term-only power series approximation,

$$g(w) = kw + \sum_{j=1}^{m} a_j w^{2j+1} \tag{11}$$

A sample "$H_{c2}$" estimate is shown in Figure 9 for $m = 6$ where it is apparent that this higher order approximation has improved the estimation of the first mode of vibration. The excessive noise that appears on the amplitude of the first mode can be suppressed with additional data averaging.

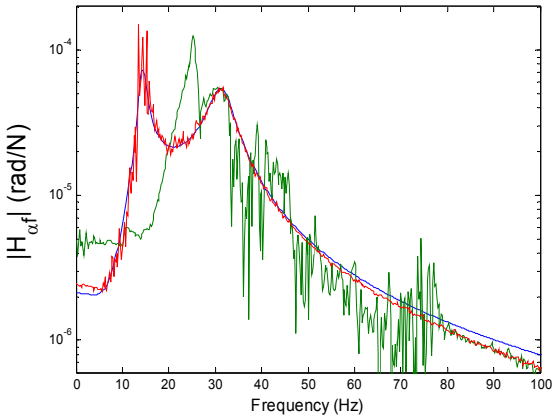


Figure 9. Magnitude of FRF of wing rotation to aileron excitation. —, actual FRF; —, conventional estimate; —, conditioned estimate using thirteenth order odd-term-only power series approximation.

## IV. Application to AAW Flight Test Data

In this section, data collected from the Active Aeroelastic Wing aircraft is used to identify an approximate underlying linear dynamic model of this aircraft by minimizing influences from aeroelastic nonlinearities. In particular, data collected during the following flight conditions are utilized: Mach = 0.5, altitude = 15,000 ft. Aileron displacement was used for excitation of the aircraft, and therefore is used as the output of the "reverse path" model. Likewise, accelerations were measured at forward and aft locations at the wing tip; therefore, these accelerations are used as the input **X** of the "reverse path" model of Figure 1(a). Since the RPSM is a frequency domain based system identification technique, selecting radix-2 sized data sets enables the computationally efficiency of the fast Fourier transform for spectral conditioning calculations. Consequently, for this analysis, an automated approach was taken for identifying the most accurate "reverse path" model from a large number of different combinations of nonlinear terms. A batch file was coded that performed the necessary calculations considering 100 different nonlinear models. To assess the accuracy of each model, the areas under the cumulative coherence functions were calculated and a plot of these areas was then used to identify the most accurate models. Of these models, the most accurate was one that included the following nonlinearities,

$$\sum_{j=1}^{3} a_j x_2^{2j+1}, \ \sum_{j=1}^{3} b_j (x_1 - x_2)^{2j+1} \qquad (12a,b)$$

where $x_2$ is the aft wing tip displacement and $x_1$ is the forward wing tip displacement. Note that since acceleration was originally measured, double integration was necessary to obtain wing tip displacements. Also, only displacement dependent nonlinearities are considered.

Figure 10 contains sample results from the most accurate model. The conditioned "$H_{c2}$" estimated frequency response between the aft accelerometer signal (displacement after the double integration) and aileron displacement reveals peaks with larger magnitudes compared with the frequency response from the conventional "$H_1$" estimate. In addition, the coherence for these two estimates indicates a more accurate "$H_{c2}$" estimate in the 5 to 9 Hz frequency range. Keeping in mind that the "$H_1$" estimate does not compensate for the presence of nonlinearities, then it is possible that the reduced magnitude in the "$H_1$" estimate is due to hardening spring structural nonlinearities of the aircraft wing (although fluid-type nonlinearities may also contribute as suggested below).

In the evaluation study of the previous section, the coefficients of the actual nonlinearities were independent of frequency. However, this is not a necessary condition. In fact, nonlinearities that exhibit memory are frequency dependent and have been seen in various physical phenomenon such as wake vortices[18]. Since the RPSM makes no assumption about the frequency dependence of the nonlinear coefficients, nonlinearities that exhibit memory are automatically identified. Figure 10(c) Illustrates the most dominant coefficient estimated where frequency dependence is apparent. This is the coefficient of the fifth order relative displacement term of equation (12b). The

coefficient's dominant frequencies coincide with the frequency response peak frequencies. Also, this coefficient is always positive over this frequency range indicating the presence of a hardening nonlinearity as previously suggested. Note, the magnitude of this coefficient is in the order of $10^{18}$ (E is prefix exa). This is not unusual since the relative response $x_1$-$x_2$ is on the order of $10^{-4}$ $m$ and when taken to the fifth power is on the order of $10^{-20}$ $m^5$. Therefore, although $b_2$ has a relatively large value the nonlinear term $b_2(x_1\text{-}x_2)^5$ is only on the order of 100 N. The frequency dependence of the estimated coefficient indicates that this nonlinearity might be the result of an aeroelastic nonlinearity with memory.

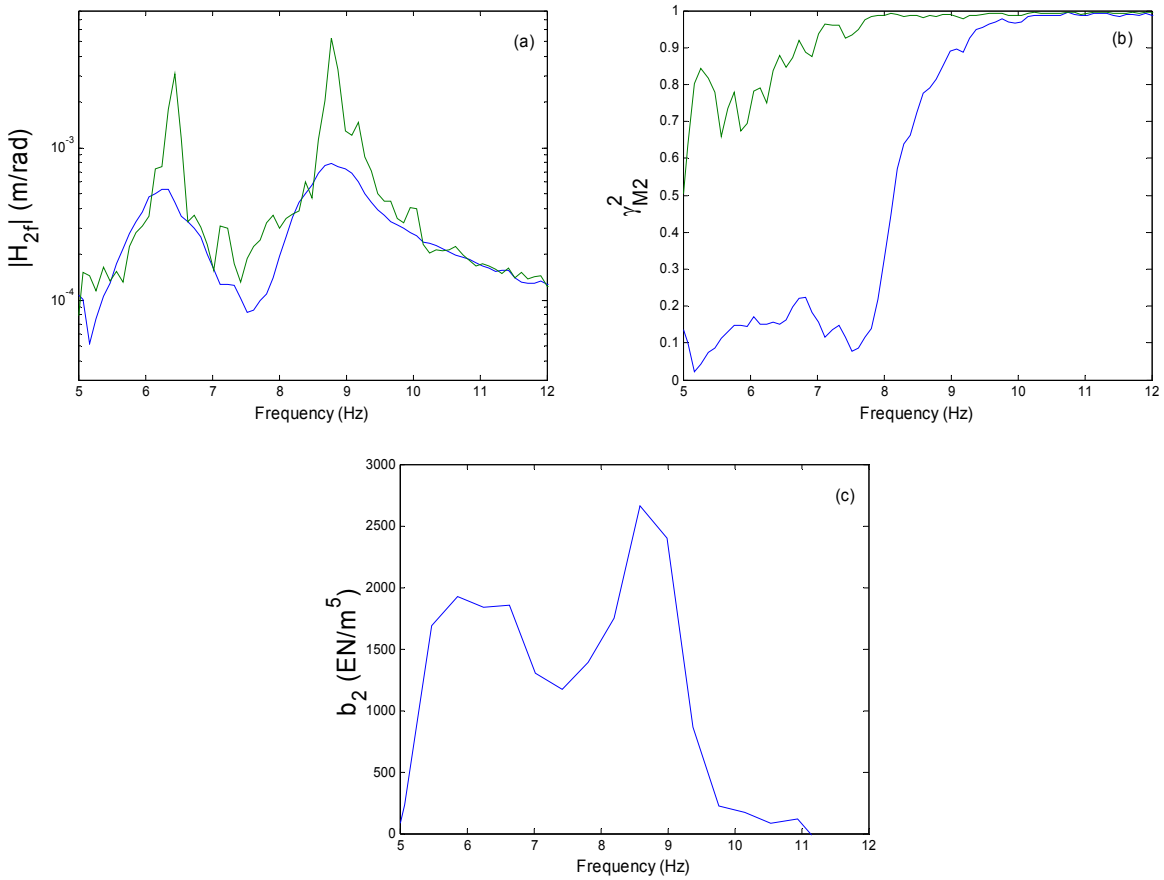


Figure 10. Frequency responses, coherences and coefficient estimate for AAW flight data. (a) Magnitude of FRFs of wing tip aft accelerometer response to aileron displacement. (b) Coherence functions for wing tip aft accelerometer response to aileron displacement. —, conventional estimate; —, conditioned estimate using model of equation (12). (c) estimate of coefficient of fifth order relative displacement term of equation (12b).

## V. Conclusions

The "Reverse Path" Spectral Method has been evaluated using a nonlinear two-degree-of-freedom aeroelastic model. The capability of identifying the nonlinear aeroelastic system even when the exact form of the nonlinearity is unknown was illustrated. Likewise, the usefulness of the cumulative coherence function (as derived from the conditioned "reverse path" model) as a utility for indicating the accuracy of the "reverse path" model was shown. When applied to Active Aeroelastic Wing flight data, the RPSM identified a model that yielded better coherence than the conventional "$H_1$" estimate of the same data. The underlying linear frequency response functions estimated by the conditioned "$H_{c2}$" method showed peaks with higher amplitudes than the peaks of the conventional "$H_1$" method. Consequently, it is likely that a hardening nonlinearity is present resulting in a suppression of the peak amplitudes. The dominant coefficient of the identified nonlinear terms was found to be frequency dependent, indicating an aeroelastic nonlinearity with memory.

The wings of the AAW are instrumented with over 250 response sensors, providing a large amount of data to be utilized for nonlinear system identification. In addition, many other experiments have been conducted under different flight conditions. Consequently, further work in the application of the RPSM for identifying a nonlinear aeroelastic model of the AAW will include the use of additional flight response data not considered here. Also, because of the recent successes of wavelets for describing nonlinear aeroelastic systems, future modification to the RPSM will include wavelet functions as inputs to the "reverse path" model.

## VI. Acknowledgement

This work was supported by the NASA Kentucky EPSCoR and the NASA Faculty Fellowship programs.

## VII. References

1. R. Lind and M. Brenner, *Robust Aeroservoelastic Stability Analysis: Flight Test Applications*, Series: Advances in Industrial Control, Springer-Verlag, 1999.
2. R. J. Prazenica, R. Lind and A. Kurdila 2003 *AIAA Journal of Guidance, Control, and Dynamics* **26**, 331-339. Uncertainty Estimation from Volterra Kernels for Robust Flutter Analysis.
3. R. Lind, R. J. Prazenica, and M. J. Brenner 2003 *Proceedings of the AIAA Structures, Structural Dynamics, and Materials Conference, Norfolk, VA*. AIAA-03-1406. Estimating Nonlinearity using Volterra Kernels in Feedback with Linear Models.
4. E. H. Dowell and D. Tang 2002 *AIAA Journal* **40**, 1697-1707. Nonlinear aeroelasticity and unsteady aerodynamics.
5. E. Dowell, J. Edwards and T. Strganac 2003 *AIAA Journal of Aircraft* **40**, 857-874. Nonlinear aeroelasticity.
6. B. H. K. Lee, S. J. Price and Y. S. Wong 1999 *Progress in Aerospace Sciences* **35**, 205-334. Nonlinear aeroelastic analysis of airfoils: bifurcation and chaos.
7. R. Lind, K. Snyder and M. Brenner 2001 *Mechanical Systems and Signal Processing* **15**, 337-356. Wavelet analysis to characterise non-linearities and predict limit cycles of an aeroelastic system.
8. M. J. Brenner 2003 *Mechanical Systems and Signal Processing* **17**, 765-786. Non-stationary dynamics data analysis with wavelet-svd filtering.
9. C. M. Richards and R. Singh 1998 *Journal of Sound and Vibration* **213**, 673-708. Identification of multi-degree-of-freedom nonlinear systems under random excitations by the "reverse path" spectral method.
10. C. M. Richards and R. Singh 1999 *Journal of Sound and Vibration* **220**, 413-450. Feasibility of identifying non-linear vibratory systems consisting of unknown polynomial forms.
11. E. W. Pendleton, D. Bessette, P. B. Field, G. D. Miller and K. E. Griffin 2000 *AIAA Journal of Aircraft* 37, 554-561. Active aeroelastic wing flight research program: technical program and model analytical development.
12. L. D. Mitchell 1982 *American Society of Mechanical Engineers, Journal of Mechanical Design* **104**, 277-279. Improved methods for the Fast Fourier Transform (FFT) calculation of the frequency response function.
13. H. R. Busby, C. Nopporn and R. Singh 1986 *Journal of Sound and Vibration* **180**, 415-427. Experimental modal analysis of non-linear systems: a feasibility study.
14. J. S. Bendat and A. G. Piersol 1986 *Random Data. Analysis and Measurement Procedures*. New York. Wiley-Interscience, second edition.
15. K. R. Godfrey, A. H. Tan and H. A. Barker 2003 *Proceedings of the 13$^{th}$ IFAC Symposium on System Identification*. A survey of readily accessible perturbation signals.
16. Rik Pintelon and Johan Schoukens 2001 System Identification: A Frequency Domain Approach. IEEE Press.
17. R. J. Allemang and D. L. Brown 1998 *Journal of Sound and Vibration* **211**, 301-322. A unified matrix polynomial approach to modal identification.
18. J. S. Bendat, R. N. Coppolino and P. A. Palo 1995 *International Journal of Non-Linear Mechanics* **30**, 841-860. Identification of physical parameters with memory in non-linear systems.